

RSC Advances



This is an *Accepted Manuscript*, which has been through the Royal Society of Chemistry peer review process and has been accepted for publication.

Accepted Manuscripts are published online shortly after acceptance, before technical editing, formatting and proof reading. Using this free service, authors can make their results available to the community, in citable form, before we publish the edited article. This *Accepted Manuscript* will be replaced by the edited, formatted and paginated article as soon as this is available.

You can find more information about *Accepted Manuscripts* in the [Information for Authors](#).

Please note that technical editing may introduce minor changes to the text and/or graphics, which may alter content. The journal's standard [Terms & Conditions](#) and the [Ethical guidelines](#) still apply. In no event shall the Royal Society of Chemistry be held responsible for any errors or omissions in this *Accepted Manuscript* or any consequences arising from the use of any information it contains.



Journal Name

ARTICLE

**Nanocomposite membrane composed of nano-alumina within sulfonated
PVDF-co-HFP/Nafion blend as separating barrier in single chambered
microbial fuel cell**

zReceived 00th January 20xx,
Accepted 00th January 20xx

DOI: 10.1039/x0xx00000x

www.rsc.org/

Vikash Kumar, Piyush Kumar, Arpita Nandy, Patit P. Kundu*

Abstract

Nano- Al_2O_3 is incorporated within the blend of sulfonated PVDF-co-HFP/Nafion in varying molar ratios for preparation of nanocomposite membranes. A series of tests namely, water uptake, swelling ratios, ion-exchange capacity (IEC), proton conductivity, oxygen diffusivity, etc. were conducted to analyze its potency in microbial fuel cell (MFC). The enhanced water uptake, proton conductivity, and oxygen diffusivity results were observed with increasing nano Al_2O_3 in the membrane. The sample A5, containing 5 wt% nano Al_2O_3 , exhibited superior proton conductivity over naive SPVdF-co-HFP (~88%) and Nafion 115 membrane (~3.5%). In addition, this prospective membrane revealed comparable ion exchange capacity and reduced oxygen diffusivity than corresponding Nafion 115. Furthermore, the electrical efficiency of this particular membrane was determined in single chambered MFCs as a constituent of membrane electrode assembly. Employing mixed *firmicutes* as biocatalysts, a maximum power and current density of $541.52 \pm 27 \text{ mWm}^{-2}$ and $1900 \pm 95 \text{ mA m}^{-2}$ were observed from MFC, which revealed an overall ~48 and 11% increase over naive SPVdF-co-HFP and Nafion 115 membrane. With marked lowering in impedance, the results indicate the relevance of Al_2O_3 filled nanocomposite as separating barrier in single chambered MFCs for microbial bio-energy conversion.

INTRODUCTION

Global energy demand, with depleting resources, calls for newer alternative technologies for sustained growth. One such way-out is “Microbial fuel cell” (MFC) which uses microbial power in harnessing bio-energy. The basic principle of MFC

is the production of electrical potential through oxidation of substrates via microorganisms, generating protons and electrons in the anode chamber, where, protons get transferred via proton exchange membrane (PEM) and electrons from

ARTICLE

Journal Name

anodic electrodes are conducted to the cathode chamber through an external circuit [1,2].

This microbial energy harvesting capacity in MFC was first demonstrated by Bennetto *et al* in the early 80's [3, 4]. Later, this brought considerable interest with efficient design and fabrication. One such essential parameter is the polymer electrolyte membrane (PEM) that influences the overall performance of MFC. Generally, any ion permeable material can function as PEM; however, its choice serves as a decisive factor in controlling the internal resistance of the system. Extensive research on membrane modification and optimization has been reported. Polymers like polystyrene, polyether ether ketone (PEEK), poly (arylene ether sulfone), phenylated polysulfone, polyphosphazenes, polyimides, poly(4-phenoxybenzoyl-1,4-phenylene), polybenzimidazole(PBI), polyolefins and polypropylene (PP) have been widely specified as raw materials for membranes [5-8]. In an instance, sulfonated polystyrene-ethylene-butylene-polystyrene (SPSEBS) and sulfonated polyether ether ketone (SPEEK) were found to be producing a respective ~ 106.9% and ~55.2% power density higher over the commercially available Nafion membrane [9-10].

Similarly, several studies on enhancing membranes properties have been conducted, for instance, polyvinylidene fluoride (PVDF) and its copolymer with varied blend compositions, IPNs and sulfonations have been reported to enhance water uptake, IEC and proton conductivity of membranes [11-18]. Other alternatives like photosulfonation, plasma treatment, radiation grafting, etc. have also been shown to alter membrane properties [19-23]. It has been reported that

membrane alone contributes to more than 38% of the overall cost in MFC [24]. Another apt way of enhancing membrane efficiency is usage of inorganic fillers as nanocomposite membranes. Rahimnejad *et al.* showed Fe₃O₄/PES nanocomposite membranes in MFCs with *Saccharomyces cerevisiae* as biocatalyst where, increased performance over conventional Nafion 117 membrane was observed [25]. The reason was attributed to the presence of Fe₃O₄ nanoparticles that enhanced conductivity with corresponding low roughness in the membranes. Likewise, the hygroscopic nature of inorganic oxides and ceramic nano fillers (>100 nm) have been found to enhance various polymeric membrane properties e.g (Nafion, PVdF, etc). The water molecules get adsorbed and stored in the voids of the nanofillers and thus, enhances water retention in the composite membranes. Other attributes like physical, thermal and electrochemical nature have also been shown to get influenced in the process [26-33].

Owing to that, here, composites of sulfonated PVDF-co-HFP (SPVdF-co-HFP)/Nafion membrane have been developed using different concentrations (5, 10 and 20 wt %) of alumina (Al₂O₃) as replacement of Nafion in 80:20 SPVdF/Nafion blend. They have been respectively named as A5, A10 and A20 where their performances are compared with Nafion 115, sulfonated PVDF-co-HFP and SPVdF-co-HFP/Nafion blend (A0) membranes in MFC. In effect, we report the preparation and characterization of low cost composite PEM material composed of nano alumina within the blend of sulfonated-PVdF-co-HFP/Nafion for application in MFC with mixed *firmicutes* as biocatalysts.

RESULTS AND DISCUSSION

Fourier Transform Infrared (FTIR) analysis

Composite membranes of nano Al_2O_3 mixed with sulfonated PVdF-co-HFP and Nafion were characterized using FT-IR spectroscopy where, the structural identities of various functional groups were featured with major peak position/intensity differences (Figure S1, Supplementary material). The corresponding IR peak intensities at 1067 cm^{-1} , 1165 cm^{-1} and 1400 cm^{-1} were assigned to the symmetrical and asymmetrical stretchings of the constituent S=O bonds of $-\text{SO}_3\text{H}$ groups [15]. Another peak at 1646 cm^{-1} revealed the presence of Al–O stretching in the composite membrane structures [34]. With increasing nano Al_2O_3 , increments in these peak intensities were found in all composite membranes (A5, A10 and A20). Relatively, the characteristic peak intensities at $500\text{--}800\text{ cm}^{-1}$ were observed in all nanocomposite membranes (A5–A20), corresponding to Al–O–Al stretching. As all these peaks were found absent in sulfonated PVdF-co-HFP membrane (SPVdF-co-HFP), the latter evidently ensured the successful incorporation of nano fillers (Al_2O_3) within the casted nanocomposite membranes. In effect, reductions in SO_3H groups were clearly disclosed with lowered peak intensities with increasing Al_2O_3 content and reduced SO_3H groups in A5–A20 membranes.

Water uptake and swelling ratio analysis

The water uptake (WU) values for the casted membranes were obtained in triplicate. Figure 1 illustrates the corresponding water uptake values for the casted

nanocomposite membranes as bar diagram. In effect, samples prepared from 80:20 SPVdF-co-HFP: Nafion without any filler (A0), with 5% Al_2O_3 (A5), with 10% Al_2O_3 (A10) and with 20% Al_2O_3 (A20) showed a respective $\sim 20.4\%$, 24%, 33% and 36% water uptake values. Enhanced water uptake capacities were observed with increasing Al_2O_3 content in the membrane. With increasing inter-space free volume, the casted membranes showed a linear rise on subsequent alumina addition. The extremely hygroscopic nature of Al_2O_3 resulted in the formation of voids with tortuous channels in the matrix structure, leading to increased water retention in the membranes.

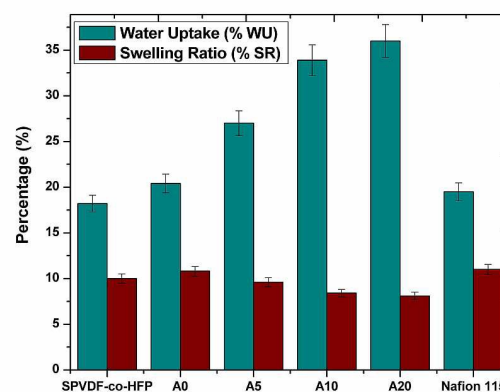


Fig 1: Water uptake and swelling ratios of the composite membranes

In accordance, the swelling properties of the membranes were calculated. The corresponding swelling results followed a reverse trend as that obtained for the water uptake capacity. The respective swelling ratios (SR) for samples A0, A5, A10 and A20 membranes were $\sim 10.8\%$, 9.6% , 8.4% and 8.1% . The gradual replacement of sulfonic groups (present in 20%

nafion) with inorganic Al_2O_3 nanofillers resulted in a decrease in the swelling ratios in the membrane. Incorporated Al_2O_3 allowed higher interfacial interaction within membrane structure that increased the overall rigidity of the membrane. Surface agglomeration of alumina resulted in pore blockages that in turn increased the nanocomposite stiffness with lowering in swelling ratios (S2, Supplementary information). Nevertheless, with reduced swelling ratios and enhanced water uptake capacities, the casted nanocomposite membranes (A5- A20) were found to be better in comparison to the naive SPVdF-co-HFP membrane.

Analysis of IEC and proton conductivity

Using titration method, membrane ion-exchange capacities (IEC) were determined, where the initially attached/ incorporated ions were displaced by an oppositely charged ion present in the medium [35]. Figure 2 represents the respective IEC and proton conductivity values of the casted membranes. The obtained respective IECs for A0, A5, A10 and A20 membranes were 0.72 meq g^{-1} , 0.66 meq g^{-1} , 0.47 meq g^{-1} and 0.27 meq g^{-1} . As we move from A0 to A20, reductions in IEC values were observed with increasing Al_2O_3 content in the membrane. The corresponding sulfonic ($-\text{SO}_3\text{H}$) groups present in Nafion were substituted with increasing Al_2O_3 content, that in turn, lowered the respective IEC values in the nanocomposite membrane. Without any nanofiller, A0 showed slightly lower IEC (0.72 meq g^{-1}) over Nafion-115 (0.81 meq g^{-1}). This was mainly because the used SPVDF-co-HFP present in the blend was not fully sulfonated as Nafion-

115. Nevertheless, in comparison to naive SPVdF-co-HFP, IECs were found higher in A0, A5 and A10 membranes due to the presence of Nafion in the blend component. In A20, Nafion was totally replaced with nanoalumina that showed least IEC amongst all the studied membranes.

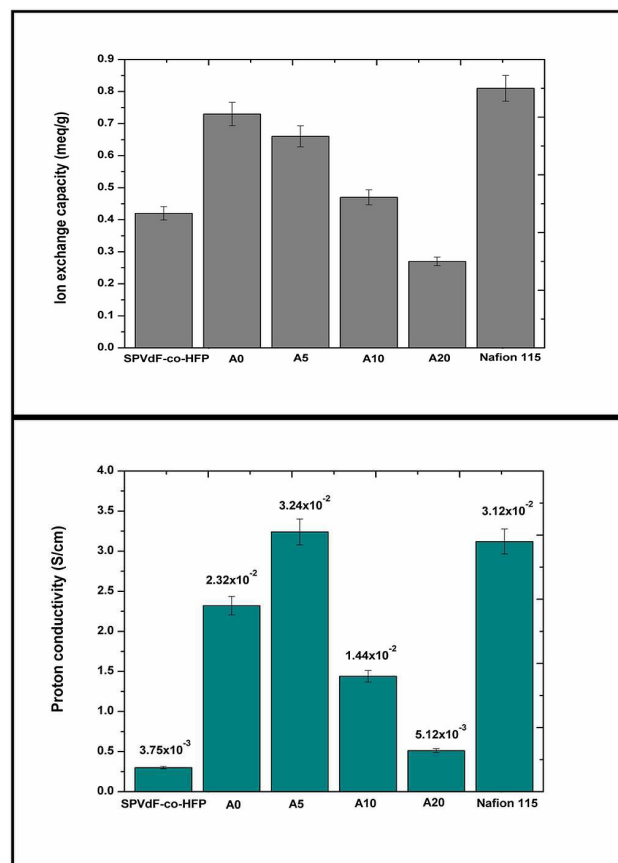


Fig 2: Ion exchange and proton conductive capacities of the membranes

Ion exchange capacity directly influences proton conductivity in membranes, which was expected to follow same course as mentioned in IECs. The trend for proton conductivity was found very similar here except for A5, which showed highest proton conductivity amongst all casted membranes. From A5, decline in proton conductivities were observed with least in A20 membrane. A respective proton conductivity of 2.32×10^{-2} , 3.57×10^{-2} , 1.44×10^{-2} and 5.12×10^{-3} were observed in A0,

A5, A10 and A20 membranes. Protons get exchanged with the available sulfonic acid groups present on the membrane, where the replacement of Nafion by nanoalumina declined IEC in the blend that resulted in decreased proton conductivity. However, increasing Al_2O_3 enhanced the water uptake capacities in membranes which aided in their respective proton conductive values. In A5, (with 5% nanoalumina loading in the blends of SPVDF-co-HFP and Nafion), the filler was mixed at the molecular level with least agglomeration and thereby the effect of water uptake attributed in higher proton conductivity, despite of lowered sulfonic ($-\text{SO}_3\text{H}$) groups in the membrane. In effect, slightly reduced IEC, but increased proton conductivity was observed in A5 over Nafion 115. For other composite membranes (A10 and A20), the reduced sulfonic ($-\text{SO}_3\text{H}$) groups with increased deposition of Al_2O_3 as clumps, resulted in lower proton conductivity in membranes. Regardless of the increased hygroscopic nature of Al_2O_3 , tortuous channels formed with excess alumina clogging, allowed higher water retention with increased stiffness, but relatively lower proton conductivity in A10 and A20 membranes. Thus, despite of their increased water uptake capacity, increased Al_2O_3 agglomeration resulted in lower proton conductivity in A10 and A20 membranes [34]. In effect, with reduced sulfonic ($-\text{SO}_3\text{H}$) groups (because of reduced Nafion content), and increased water uptake capacity (because of the increasing Al_2O_3 content) corresponding variations in nano composite membranes were observed. Nevertheless, in spite of these reductions, proton conductivity of A20 was found approximately ~26% higher over naive SPVDF-co-HFP

membrane. In comparison, A5 showed an approximate ~3.9% increased proton conductivity over Nafion 115 membrane. In general, the obtained water uptake capacities with corresponding IEC and proton conductivities indicated positive effect of incorporated nano Al_2O_3 in all casted nanocomposite membranes.

MFC performance

For initial potential build up, MFCs were kept devoid of external resistances, where the air facing side of cathode was masked with parafilm to establish a favourable anodic start-up condition. The systems were left undisturbed for voltage build-up and acclimatization. Taking Ag/AgCl as reference, an average anode and cathode potentials of -225 mV and +171 mV were observed with mild fluctuations (data not shown here). With sustenance, gradual OCV (open circuit voltage) increments were observed in MFCs which varied from ~0.6 to 0.75 Volts. MFC-D (with fitted A5 membrane) was observed with highest OCV amongst all employed units with approximately ~741±20 mV in succession (Figure 3).

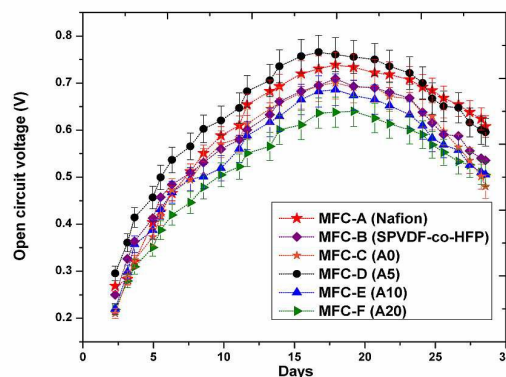


Fig 3: Open circuit potentials in respective MFCs

The enhanced cell efficiencies showed increased voltage drops in MFCs, with a maximum current of 1.07 mA, 0.82 mA, 1.03 mA, 1.14 mA, 0.98 mA, and 0.94 mA from MFC A to F respectively. (S3, Supplementary information). In accordance, MFC-D with A5 membrane showed increased cell performance over other employed units. The reason was attributed to its higher proton conductivity that aided in enhanced performance in MFC-D. In comparison, lower efficiency from A10 and A20 were observed, mainly due to the agglomeration of increased Al_2O_3 on membrane surface that formed tortuous channels in the membranes with excess alumina clogging. Thus, despite of higher water retentions, relatively lower proton conductivity and IECs were observed in A10 and A20 membranes with increased stiffness. This reduced IEC and proton conductivity allowed hindered cell performances in MFC-E and F with reduced OCV and currents over other employed units. Cell performances evidently distinguished the efficiency of the employed membranes, where MEA effect was considered as a crucial factor (in diminishing the electrolyte resistance) and thus, increasing the overall systemic efficacy [36, 37].

Electrochemical impedance spectroscopic (EIS) analysis

To measure the internal resistance (R_{in}), MFCs were given a two mode setup. Anode as working, whereas, reference and counter terminals were connected to the cathode. Figure 6 shows the respective nyquist plots for each MFC. These were used to calculate the specific resistive components of MFCs, segmenting them as shown in equivalent circuit (Figure 4). Internal resistance (R_{in}) of the whole system is generally

divided as activation resistance, ohmic resistance (R_m attributed to electrode resistance, membrane resistance, etc.) and concentration resistance [38]. The ohmic resistances (R_m) were found inversely proportional to the alumina content in the membranes. A respective R_m (Figure 5) of $\sim 6.36\Omega$ for MFC-A, $\sim 12.57\Omega$ for MFC-B, $\sim 9.82\Omega$ for MFC-C, $\sim 5.73\Omega$ for MFC-D, $\sim 4.62\Omega$ for MFC-E, and $\sim 3.27\Omega$ for MFC-F were observed, indicating nano-alumina effect on membranes.

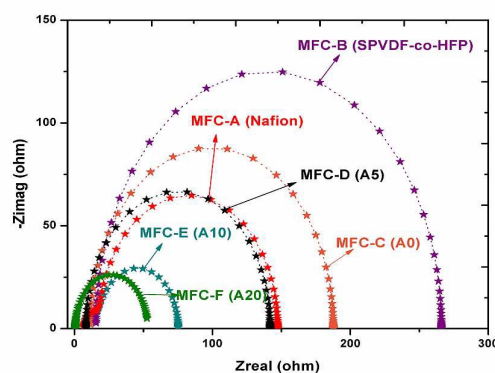


Fig 4: Electrochemical impedance spectroscopy (EIS) of MFCs

Alumina incorporation showed increased membrane polarity in fitted A20 and A10 membranes that resulted in minimal impedance in MFC-F and E units. In comparison, relatively higher ohmic resistances were observed in MFC-B and C with fitted SPVdF-co-HFP and A0 membranes. This was expected, as SPVdF-co-HFP and A0, being relatively pristine, were having relatively lower water uptake that showed increased ionic hindrance in the system.

MFC-D, on the other hand showed relatively higher impedance in comparison to MFC-E and F (with A10 and 20 membranes), which were indicative of its lower alumina

content (in A5 membrane). However, this was slightly lower than MFC-A (with Nafion 115 membrane). The enhanced ionic flow indicated the effect of nano-alumina incorporation in membrane, where increased water uptake influenced the higher mass transfer that relatively allowed lower impedance across the casted nano-composite membranes. As an effect, lower ohmic resistances in A20 and 10 membranes were observed, indicating reduced systemic impedance in MFC-E and F over other employed units.

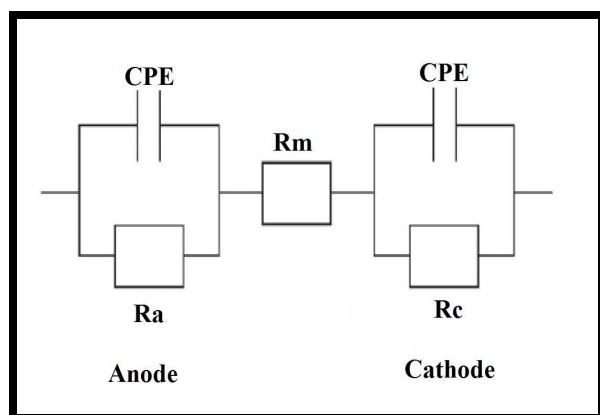


Fig 5: Equivalent circuit representing ohmic resistance (R_m)

Polarization

Polarization curves were obtained using multiple external resistors (10^7 - 10Ω) in descending range (Figure 6). With reference electrode, anode potentials were obtained and the respective cathode potentials were calculated by subtracting the anode potentials from the cell voltage. Here, increased activation losses with frequent voltage drops were observed at higher resistances. This was indicative of the energy lost in initiating the redox reaction, i.e., charge transfer from microbe to the anode surface. At lower resistances, higher voltage drops were observed, indicating ease in electron flow

within the circuit. The relatively higher proton conductivity of A5 showed approximately $\sim 11\%$ higher performance over fitted Nafion115 membrane in MFC-A. In effect, MFC-D with employed A5 membrane showed a highest power density of $541.52 \pm 27 \text{ mWm}^{-2}$ at a respective current density of $1900 \pm 95 \text{ mA} \cdot \text{m}^{-2}$.

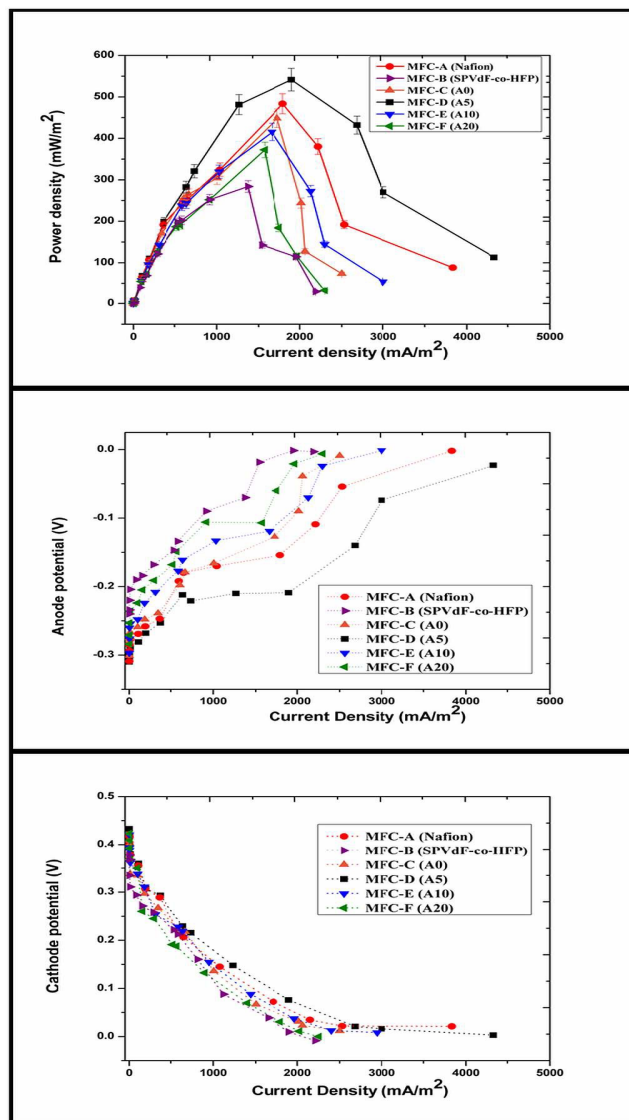


Fig 6: Polarization curves of MFCs

In addition, a respective power and current densities of $483.48 \pm 24 \text{ mWm}^{-2}$ and $1795.33 \pm 89 \text{ mA} \cdot \text{m}^{-2}$ (in MFC-A

with Nafion 115), $283.73 \pm 14 \text{ mWm}^{-2}$ and $1375.39 \pm 68 \text{ mAm}^{-2}$ (in MFC-B with SPVdF-co-HFP), $448.24 \pm 22 \text{ mWm}^{-2}$ and $1728.67 \pm 86 \text{ mAm}^{-2}$ (in MFC-C with A0), $415.43 \pm 20 \text{ mWm}^{-2}$ and $1664.42 \pm 83 \text{ mAm}^{-2}$ (in MFC-E with A10) and $372.25 \pm 18 \text{ mWm}^{-2}$ and $1576.33 \pm 78 \text{ mAm}^{-2}$ (in MFC-F with A20) were observed from individual MFCs. Comparing the performance, MFC-D showed an approximate $\sim 48\%$, 18% , 23% , and 31% higher power density over other employed units (MFC B-F).

With increased water uptake capacity, alumina incorporation had both, advantages as well as disadvantages in the membrane property. In case of 5% incorporated nano-alumina, higher IEC and proton conductivities were observed. This relatively showed increased negative potentials at anode, indicating enhanced MFC-D performance with A5 membrane. Also, the cathodic performances at lower and higher current density ranges showed enhancements in MFC-D performance over other employed units. On the contrary, excess alumina (10-20%), showed increased mass transfer with higher water uptake capacity that resulted in lower OCVs with increased cross potentials in A10 and 20 membranes. As a consequence, lower impedances were observed in MFC-E and F. However, despite of this, lower cell performances were observed in A10 and 20 membranes, where the anodic potentials showed rapid decline towards more positive potentials, indicating relatively poor performances in MFC-E and F. The reason was attributed to the lower IEC and proton conductivity of A10 and 20 membranes that along with increased mass transfer,

contributed to approximately 8- 17% reduced performance in MFC-E and F over MFC-C (with fitted A0 membrane). Nevertheless, in comparison to SPVDF-co-HFP membrane, higher cell outputs were observed with approximately $\sim 32\%$ rise in A10 and A20 membranes, indicating the positive effects of alumina incorporation on membrane efficiency. The obtained results here were compared with other materials (e.g., SPEEK/PES, SPVDF-co-HFP, sulfonated PE/ poly styrene-DVB), to indicate the effectiveness of SPVDF-co-HFP/Nafion nanocomposite membrane in MFC application (T1, Supplementary Information). However, other system parameters like anolyte, microbes and electrode configurations (like MEAs) could also be taken in account, featuring the relevance of incorporated alumina in sulfonated PVdF-HFP /Nafion blend as a cost effective alternative PEM in MFC applications.

Oxygen diffusivity and chemical oxygen demand (COD) analysis

To study the oxygen diffusivity across membranes, periodic analysis on dissolved oxygen contents were analyzed at anode. Figure 7 indicates the diffused oxygen content from cathode to anode across the employed membranes. Increasing oxygen flux ensued a respective mass transfer coefficient of $2.4 \times 10^{-4} \text{ cm s}^{-1}$, $3.24 \times 10^{-6} \text{ cm s}^{-1}$, $8.43 \times 10^{-5} \text{ cm s}^{-1}$, $9.27 \times 10^{-4} \text{ cm s}^{-1}$, $2.16 \times 10^{-3} \text{ cm s}^{-1}$, $4.17 \times 10^{-2} \text{ cm s}^{-1}$ from Nafion 115, SPVdF-co-HFP, A0 (80:20 PVdF-do-HFP: Nafion), A5 (with 5% Al_2O_3), A10 (10% Al_2O_3) and A20 (20% Al_2O_3) membranes. With increasing alumina content, increased mass transfer were observed in the membranes, where A20 showed

maximum oxygen diffusion across MEA. The reason was attributed to the increased void space in membranes, generated due to the inorganic (alumina) and organic (polymer) inter-space that allowed more oxygen to diffuse into anode.

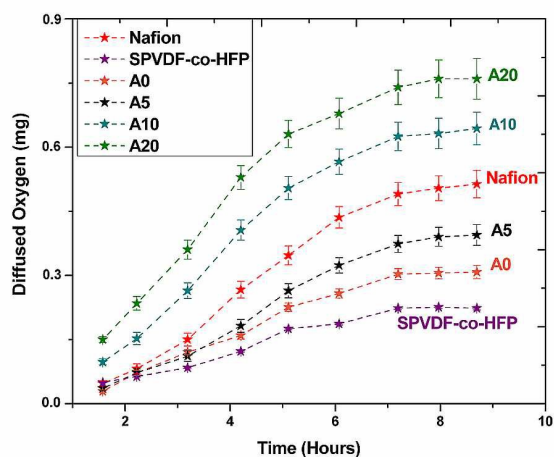


Fig 7: Oxygen diffusion across the membranes

In contrast, SPVdF-co-HFP and A0 membranes were observed with minimal oxygen diffusion. Membrane A5, containing 5% alumina nano-filler, showed reduced mass transfer in comparison to Nafion, which corresponded with an approximate ~22% lower oxygen diffusion. Approximately, 42%, 57%, 75%, and 81% increased mass transfers were observed with A0, A5, A10 and A20 membranes over naive SPVdF-co-HFP membrane. Increased oxygen permeation acts as a limitation in fuel cell that allows direct substrate oxidation without usage. Figure 8 depicts the relative % COD removals from the respective MFCs. In overall, approximately ~88.57%, ~80.39%, ~81.15%, ~86.62%, ~90.03% and ~92.67% COD removals were observed in MFC A-F respectively. The variations were primarily indicative of

the individual employed membranes in the units, where MFC-F and E with highest COD removal showed increased substrate exhaustion at anode.

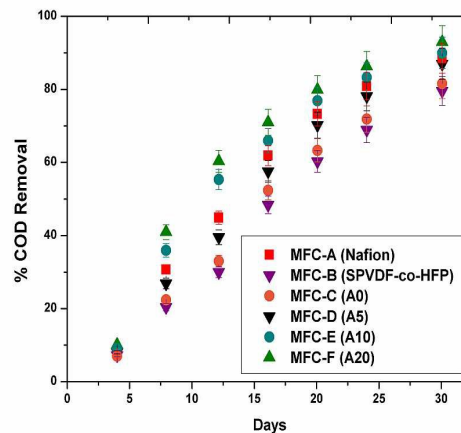


Fig 8: COD removal from MFCs

Irrespective of the current drawn out of the system, higher oxygen diffusion (across A20 and A10 membranes) showed enhanced COD removals in MFC-E and F. In comparison, lower COD removals were observed in MFCs A-D, with minimal in case of MFC-B (with SPVdF-co-HFP membrane) which corresponded with its lower ionic conductivity with increased cell impedance. Generally, COD removal is largely influenced by the employed microbes, as it is necessary to keep them electrogenetically active for sustained substrate utilization. The employed firmicutes (S4 and S5, Supplementary information) were found electrogenic that showed direct involvement in substrate utilization for bio-energy generation. In order to confirm the microbial adhesion on electrode, small portion of anode with bio-film (fixed with glutaraldehyde) were subjected for microscopic analysis (S6, Supplementary information). Figure 9 shows the images of

the microbial colonization, which revealed prominent microbial association at electrode's surface.

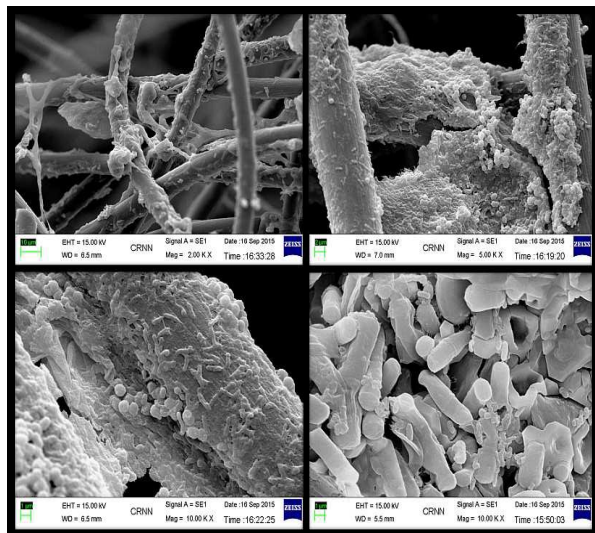


Fig 9: Scanning electron microscopic (SEM) images of microbes at anode.

Microbial metabolism serves as a decisive factor in MFCs, which affects the overall substrate utilization as several fermentative and methanogenic reactions predominates in the system, where oxygen diffusivity becomes the major concern in harnessing the available bio-energy [39-42]. In accordance, higher coulombic efficiencies (~2.8-3.3%) were observed from MFC A, C and D with respect to MFC-B, E and F (~1.8-2.3%) (Figure 10). These were primarily due to the employed membranes that showed inverse relation with respect to the diffused oxygen at anode. In effect, COD removals were inversely proportional to the coulombic efficiencies (CE), where despite of increased COD, reduced cell performances were observed in MFC-E and F (with respective A10 and 20 membranes). The plausible reasons were the direct substrate oxidation that showed increased COD removals with higher oxygen diffusions in MFC-E and F, thus resulting in lower CE and respective cell performances. In addition,

comparatively reduced CE was observed in SPVdF-co-HFP membrane, despite of its lower mass transfer over A0, A5 and Nafion membranes,. The reason was attributed to its relatively lower proton conductivity and increased impedance that limited the overall performance in MFC-B.

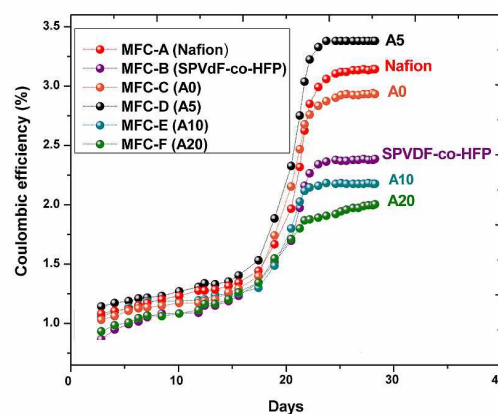


Fig 10: Coulombic efficiency of membranes

In relation, the coulombic efficiencies in A0 and A5 membranes were found enhanced, relative to their corresponding higher proton conductivities. However, in comparison to Nafion, slightly lower CE was observed in A0 membrane, which was expected, as the reduced sulfonic groups in A0, resulted in lower cell efficiency with higher cell impedance. Considering it nearly comparable to Nafion, the corresponding lower oxygen diffusivity in A0 was found relatively indicative of its higher coulombic efficiency over other employed membranes.

In effect, with higher water uptake and increased proton conductivity, the promising potential of alumina nano fillers (~5 wt %) in partially sulfonated PVdF/Nafion blends can emphatically be presented as efficient nano-composite PEM in future bio-electrochemical applications.

MATERIALS AND METHODS**General Conditions**

All chemicals of analytical and biochemical grade were used. PVdF-co-HFP (Mw-455,000), Nafion resin, NMP (1-methyl-2-pyrrolidone), chlorosulfonic acid and Al₂O₃ (≥ 50nm particle size) were obtained from Merck Millipore, India. All microbial experiments were performed under strict sterile conditions. Microbial cultures and feed transfers in MFCs were performed under laminar air flow hood to avoid contaminations with sterile air.

Membrane preparation

The sulfonation of PVdF-co-HFP was conducted with chlorosulfonic acid for 7 hours at 60°C, as reported earlier [18]. Later, it was neutralized with 1, 2 dichloroethane and named as SPVdF-co-HFP membrane with 30% sulfonation. Further, it was allowed to dissolve in NMP, where nafion resin in varied amount was added drop wise in the solution. In this homogenized blend solution, different concentrations (5%, 10%, 20%) of nano-Al₂O₃ (≥50nm) fillers were added. The casted membrane thicknesses were maintained in a range of ~200-205 μm and were kept overnight at 80°C. These were named A0 (0% Al₂O₃), A5 (5% Al₂O₃), A10 (10% Al₂O₃) and A20 (20% Al₂O₃) as shown in table 1.

Table 1: Membrane characteristics

Samples	S-PVdF-co-HFP (wt %)	Nafion(wt %)	Al ₂ O ₃ (wt %)
SP-7	100	-	-
A0	80	20	-
A5	80	15	5
A10	80	10	10
A20	80	-	20

These were further subjected for characterization such as infra red spectroscopy (FT-IR), water uptake, swelling ratio, ion exchange capacity (IEC), proton conductivity and oxygen diffusivity analysis, as described earlier [43].

Water uptake and swelling study

The dry and wet weights of membranes were used for water uptake calculation:

$$\text{Water uptake (\%)} = (W_{\text{wet}} - W_{\text{dry}}) (100) / W_{\text{dry}} \quad (1)$$

Where, W_{wet} and W_{dry} represent the weight of respective wet and dry membranes obtained after soaking in DI water for 24 hrs,

Similarly, the swelling ratios of the membranes were calculated from the following equation:

$$\text{Swelling Ratio (\%)} = (T_{\text{wet}} - T_{\text{dry}}) (100) / T_{\text{dry}} \quad (2)$$

Where, T_{wet} and T_{dry} represent the thicknesses of respective wet and dry membranes obtained after soaking in DI water for 24 hours.

Ion exchange capacity (IEC)

For measuring ion exchange capacities (IECs), titrimetric analyses of the respective membranes were conducted. Membranes were soaked overnight in 1 M H₂SO₄ solution, where excess H₂SO₄ was removed by rinsing with DI water. The samples were again soaked in 50 mL (1M NaCl solution) overnight, in order to allow replacement of protons with sodium ions. The remaining solution was neutralized with 0.01 N NaOH solution, using phenolphthalein as indicator.

The IEC value (in meq g⁻¹) was calculated as:

$$\text{IEC} = (V_{\text{NaOH}}) (S_{\text{NaOH}}) / W_{\text{dry}} \quad (3)$$

Where, V_{NaOH} , S_{NaOH} denoted the volume and strength of NaOH used in the titration, and W_{dry} was the dry weight of the membrane in gm.

Proton conductivity

To measure the conductivity of membrane, AC impedance spectroscopy was employed in transverse direction at a frequency range of 1 Hz to 10^5 Hz of 10 mV amplitude (Gamry Reference-600) (S6, Supplementary information). The conductivities of the samples (σ) were calculated from the Nyquist data, using the following equation:

$$\sigma = T/R.A \quad (4)$$

where, T is the thickness of the sample, A is the cross-sectional area of the sample, R is the resistance derived from the lower intercept of the high frequency semi-circle on a complex impedance plane with the real (Z) axis.

Membrane electrode assemblies (MEAs)

Prior MEA preparation, membranes were pre-treated with a solution mixture of 3M H_2SO_4 and water (7:3). Carbon cloths (6 cm^2) (Zoltek pvt.Ltd, USA) were used as electrodes, which were kept overnight in de-ionized water to remove any unwanted interfacial ionic particle. This also helped in maintaining electrode's total surface positivity for rigorous microbial attachment. A catalyst mixture of 10:90 wt% (Pt/C) with 5% nafion was sonicated for 30 minutes. The resulting ink was paint coated on the cathode side of the carbon cloth. A total of 3 mgcm^{-2} of supported metal catalyst was loaded on the air facing side of cathode. In total, six set of sandwiched

membranes (Nafion 115, SPVdF-co-HFP, A0, A10 and A20) between carbon cloths electrodes (as anodes and cathodes) were assembled and hot pressed at $130 \text{ }^\circ\text{C}$ for 25 seconds at 6.84 MPa pressure., This optimum condition was optimized for perfect MEA assembling, as on higher ranges, the carbon fabric became brittle and lost its texture.

Oxygen Diffusivity Measurement

The mass transfer coefficient k (cm s^{-1}), as characterized by oxygen permeability was calculated from cathode to anode chamber over time, using the mass balance equation

$$k \frac{V}{A} = -V / At \ln [C_s - C / C_s] \quad (5)$$

Where, V is the anode chamber volume, A is membrane cross-sectional area, C is the anode oxygen concentration, and C_s is cathode oxygen concentration (assumed to be the saturation concentration of oxygen in water, or 7.8 mg L^{-1}). Oxygen concentrations were measured using a dissolved oxygen probe (Horiba Pvt. Ltd, Kyoto Japan) in the anode chamber. Prior to measurement, the water was purged with purified N_2 gas for the removal of dissolved oxygen and thereafter, the concentration of dissolved oxygen was periodically recorded to observe oxygen diffusivity.

MFC Configuration and Fabrication

Six single chambered identical MFC units of 150mL liquid volume (anode chamber) containing Nafion 115, SPVdF-co-HFP, A0, A10 and A20 as MEAs were named as MFC-A, B, C, D, E and F respectively (Figure 11). For oxygen reduction, the catalyst loaded air facing side of cathode was kept facing outward. Other requisite fabrications e.g. inlet/outlet sealing,

electrode fixing, electrical connections etc were done accordingly.



Fig 11: Membrane electrode assemblies (MEA) in single chambered MFCs

Microbes and anolyte preparation

Genomic DNA of pure microbial strains was isolated using standard phenol-chloroform method [44]. Universal primers Y1Forward (40th) 5'-TGGCTCAGAACGAACGCGGCGGC-3' and Y2Reverse (337th) 5'-CCCACTGCTGCCTCC CGTAGGAGT-3' were used for 16S rRNA gene amplification by polymerase chain reaction (PCR) (Applied biosystem, US). For identification of bacterial species, sequencing and BLAST tools were employed with allotted accession numbers.

The isolated microbes were facultative anaerobes (as tested for viability in gas pack jar) of *Firmicute* class *lysini bacillus* species (EMBL accession no. HE648059, HE648060, HF548664). These mixed microbial strains were suspended in

50 mM phosphate buffer (50ml volume) and subsequently transferred to 100 ml synthetic wastewater (pH~6.9). The COD composition of the feed wastewater was $2400 \pm 150 \text{ mg l}^{-1}$ (total nitrogen: $126 \pm 33 \text{ mg l}^{-1}$, $\text{PO}_4\text{-P}$: $36 \pm 9 \text{ mg l}^{-1}$, MgSO_4 : 54 mg l^{-1}). A final volume of 150 ml (with microbe) anolyte was used as feed in MFCs.

MFC start-up, electrical parameters and measurements

Initially, all MFC units were assembled and kept sterilized with de-ionized water. Further, these were later replaced with anolyte using peristaltic pump. The units were periodically monitored (24 h intervals) using a multimeter (Keithley Instruments, Cleveland, OH, USA), and potentiostat (G600; Gamry Instrument Inc., Warminster, PA, USA), connected to a personal computer. Sequentially, current (I) and potential (V) measurements were recorded after allowing the circuit to stabilize for 8-10 minutes. The measurements were done in triplicate. Power densities (mW/m^2) were calculated by dividing the obtained power by anode surface area (6 cm^2).

Chemical oxygen demands (COD) were analyzed periodically at 420 nm (Anatech Labs India Pvt. Ltd., India) for each MFC unit. The Coulombic efficiency (CE) of the fed-batch mode MFCs were calculated as [45] applying the following formula:

$$\text{CE} = \frac{M \int_0^t I dt}{F b V_{\text{an}} \Delta \text{COD}} \quad (6)$$

where 'M' represents the molecular weight of oxygen ($M = 32$), 'F' is Faraday's constant, 'b' denotes the number of electrons exchanged per mole of oxygen ($b = 4$), ' V_{an} ' is the liquid volume in anode, and ΔCOD is the change in the chemical oxygen demand over time t.

Electrochemical impedance spectroscopy (EIS)

Potentiostatic EIS was performed at a frequency range of 10^3 kHz to 1 mHz (10 mV amplitude) for measuring the internal resistance of the unit. Nyquist graphs were plotted and the internal resistances (R_{in}) were determined for all MFCs [38].

Scanning Electron Microscopy (SEM)

The dried samples were sputter coated under vacuum with a thin gold layer. 2.5% glutaraldehyde with 0.1 M phosphate buffer solution was used to fix the biofilm, which were subsequently dehydrated with 30% to 100% ethanol [46]. Finally, these were analyzed under scanning electron microscope (Carl Zeiss EVO[®] 18 electron microscope) with an acceleration voltage of 15 kV.

CONCLUSION

In summary, varied weight percentages of nano- Al_2O_3 fillers (5%, 10%, and 20%) in SPVdF-co-HFP/Nafion blends were compared as nanocomposite MEA in single chambered MFCs, using mixed *firmicutes* as biocatalysts. Increasing Al_2O_3 concentration upto 5 wt% showed improved water uptake and proton conductivity in the membrane, where lower mass transfer in MFC resulted in higher CE over Nafion 115 membrane. The reason was attributed to the lower oxygen diffusion across 5wt% nano- Al_2O_3 incorporated membrane that revealed a maximum power and current density of $541.52 \pm 27 \text{ mWm}^{-2}$ and $1900 \pm 95 \text{ mA}m^{-2}$ in MFC. Comparing the performance, approximately ~ 11 and 48% higher power outputs were observed from 5wt% nano- Al_2O_3 over sulfonated PVdF-co-HFP and Nafion 115 membranes. Being

a cost effective approach, the results clearly indicate the efficacy of nano- Al_2O_3 incorporated SPVdF-co-HFP/Nafion membrane in MFC application. However, increasing Al_2O_3 content showed higher oxygen diffusion with minimal internal resistance that eventually served as a drawback with lower CE in MFCs. This remains another area where mass transfer lowering would rationalize its better suitability in a future bio-electrochemical applications. MFC being a future technology, demands more profound investigations in such diversified areas of membrane technology for relevant cost efficient practical alternatives.

ACKNOWLEDGEMENTS

The financial research aid provided from Council of Scientific and Industrial Research (CSIR) and Department of Science and Technology (DST) is duly acknowledged.

Notes and References

Notes

Advanced Polymer Laboratory, Department of Polymer Science & Technology, 92 A. P. C. Road, University of Calcutta, Kolkata-700009.

**Corresponding author Fax & Tel: 91-33-2352-510;*

E-mail: ppk923@yahoo.com

The authors declare no competing financial interest.

References

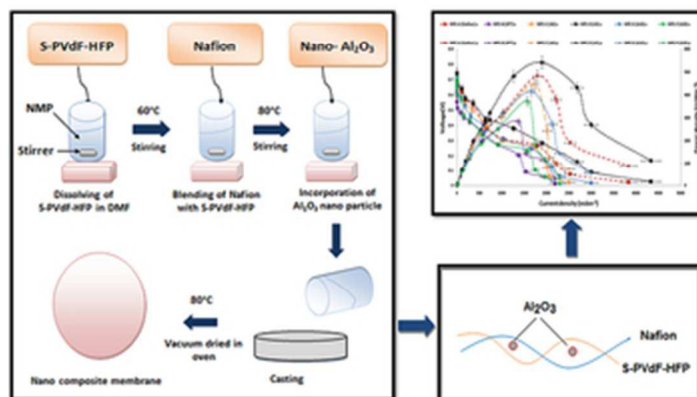
1. D. L. Hoskins, X. Zhang, M. A. Hickner and B. E. Logan, *Bioresour. Technol.*, 2014, 172, 156–161
2. Y. Hou, K. Li, H. Luo, G. Liu, R. Zhang, B. Qin and S. Chen, *Environ. Sci. Eng.*, 2014, 8, 137–143.
3. H.P. Bennetto, J.L. Stirling, K. Tanaka and C.A. Vega, *Biotechnol Bioeng*, 1983, 25, 559-568.
4. R.M.Allen and H.P.Bennetto, *Appl Biochem Biotechnol*, 1993, 39, 27-40.
5. H. Zhang and P. K. Shen, *Chem. Rev.*, 2012, 112, 2780–2832.
6. J. Yang, P. K. Shen, J. Varcoe and Z. Wei, *J. Power Sources*, 2009, 189, 1016–1019.
7. L. A. Diaz, G. C. Abuin and H. R. Corti, *J. Membr. Sci.*, 2012, 411–412, 35–44.
8. L. A. Neves, J. Benavente, I. M. Coelho and J. G. Crespo, *J.Membr. Sci.*, 2010, 347, 42–52.
9. S. Ayyaru, P. Letchoumanane, S. Dharmalingam and A. Stanislaus, *J. Power Sources*, 2012, 217, 204–208.
10. S. Ayyaru and S. Dharmalingam, *Bioresour Technol*, 2011,102, 11167–11171.
11. K. Dutta, S. Das, P. Kumar and P. P. Kundu, *Appl. Energy*,2014, 118, 183–191.
12. C. W. Lin, R. Thangamuthu and C. J. Yang, *J. Membr. Sci.*,2005, 253, 23–31.
13. P. Kumar, S. K. Jagwani and P. P. Kundu, *Materials Today Communications*, 2015, 2, e1–e8.
14. F. Liu, N. A. Hashim, Y. Liu, M. R. M. Abed and K. Li, *J.Membr. Sci.*, 2011, 375, 1–27.
15. P. Kumar, K. Dutta and P. P. Kundu, *Int. J. Energy Res.*, 2014,38, 41–50.
16. P. P. Kundu, B. T. Kim, J. E. Ahn, H. S. Han and Y. G. Shul, *J.Power Sources*, 2007, 171, 86–91.
17. M. K. Song, Y. T. Kim, J. F. Fenton, H. R. Kunz and H. W. Rhee, *J. Power Sources*, 2003, 117, 14–21.
18. S. Das, P. Kumar, K. Dutta and P. P. Kundu, *Appl. Energy*,2014, 113, 169–177.
19. H. Wang, S. J. Chen and J. Zhang, *Colloid Polym. Sci.*, 2009,287, 541–548.
20. M. Kaneko and H. Sato, *Macromol. Chem. Phys.*, 2004, 205,173–178.
21. M. Kaneko and H. Sato, *Macromol. Chem. Phys.*, 2005, 206,456–463.
22. M. Kaneko, S. Kumagai, T. Nakamura and H. Sato, *J. Appl.Polym. Sci.*, 2004, 91, 2435–2442.
23. J. Ihata, *J. Polym. Sci., Part A: Polym. Chem.*, 1988, 26, 177–185.
24. M. Ghasemi, W.R.W. Daud, S.H.A. Hassan, S. E. Oh, M. Ismail, M. Rahimnejad, J.M. Jahim, *J. Alloys Compd.*, 2013, 580, 245-255.
25. M. Rahimnejad, M. Ghasemi, G.D. Najafpour, M. Ismail, A.W. Mohammad, A.A. Ghoreyshi, S.H.A. Hassan, *Electrochim. Acta*, 2012, 85, 700-706.
26. P. Bebin, M. Caravanier and H. Galiano, *J. Membr. Sci.*, 2006, 278, 35–42.
27. Y. T. Kim, K. H. Kim, M. K. Song and H. W. Rhee, *Curr. Appl.Phys.*, 2006, 6, 612–615.
28. S. Ren, G. Sun, C. Li, S. Song, Q. Xin and X. Yang, *J. Power Sources*, 2006, 157, 724–726.

ARTICLE

Journal Name

29. S. Licoccia and E. Traversa, *J. Power Sources*, 2006, 159, 12–20.
30. S. Rao, R. Xiu, J. Si, S. Lu, M. Yang and Y. Xiang, *ChemSusChem*, 2014, 7, 822–828.
31. G. E. J. Poinern, N. Ali and D. Fawcett, *Materials*, 2011, 4, 487–526.
32. Z. Ghezelbash, D. Ashouri, S. Mousavian, A. H. Ghandi and Y. Rahnama, *Bull. Mater. Sci.*, 2012, 35(6), 925–931.
33. B. Kumar and J. P. Fellner, *J. Power Sources*, 2003, 123, 132–136.
34. P. Kumar, A. D. Singh, V. Kumar and P. P. Kundu, *RSC Adv.*, 2015, 5, 63465-72.
35. J.D. Jeon and S.Y. Kwak, *J Phys Chem B*. 2007, 111, 9437–43.
36. A. ElMekawy, H. Hegab, X. Dominguez-Benetton and D. Pant, *Bioresour Technol.* 2013, 142, 672–82.
37. F. Zhang, Y. Ahn and B. E. Logan, *Bioresour. Technol.*, 2014, 152, 46–52
38. Z.He and F.Mansfeld, *Energy Environ Sci*, 2009, 2, 215–9.
39. A. ElMekawy, H. Hegab and D. Pant, *Energy Environ Sci*. 2014, 7, 3921-33.
40. B.Min , J.Kim , S.Oh , J.M.Regan and B.E.Logan, *Water Res* 2005, 39, 4961–8.
41. Z.He, S.D.Minteer and L.T.Angenent, *Environ Sci Technol*, 2005, 39, 5262–7.
42. J.Greenman, A.Ga'livez, L.Giusti and I.Ieropoulos, *Enzyme Microb Technol*, 2009, 44,112–9.
43. R. Rudra, V. Kumar and P. P. Kundu, *RSC Adv.*, 2015, 5, 83436-47.
44. A.Ghosh, B.Maity, K.Chakrabati and D.Chattopadhyay, *Microb Ecol*, 2007, 54, 452-459.
45. V. Kumar, P. Kumar, A. Nandy and P. P. Kundu, *RSC Adv.*, 2015, 5, 30758-67.
46. S. Xu and H.Liu, *J Appl Microbiol*, 2011,111, 1108-15.

Graphical Representation



29x20mm (300 x 300 DPI)